

Hybrid stars in the light of GW170817

Rana Nandi*

Tata Institute of Fundamental Research, Mumbai - 400005, India

Prasanta Char†

Inter-University Centre for Astronomy and Astrophysics,

Post Bag 4, Ganeshkhind, Pune - 411 007, India

Abstract

We have studied the effect of tidal deformability constraint given by the binary neutron star merger event GW170817 on the equations of state (EOS) of hybrid stars. The EOS are constructed by matching the hadronic EOS described by RMF model and parameter sets NL3, TM1 and NL3 $\omega\rho$ with the quark matter EOS described by modified MIT bag model, via Gibbs' construction. It is found that the tidal deformability constraints along with the lower bound on maximum mass ($M_{\max} = 2.01 \pm 0.04M_{\odot}$) significantly limits the bag model parameter space ($B_{\text{eff}}^{1/4}, a_4$). We also obtain upper limits on the radius of of $1.4M_{\odot}$ and $1.6M_{\odot}$ stars as $R_{1.4} \lesssim 13.7 - 13.9$ km and $R_{1.6} \lesssim 13.3$, respectively.

* rana.nandi@tifr.res.in

† pchar@iucaa.in

I. INTRODUCTION

We have just entered the era of multi-messenger astronomy with the simultaneous detections of gravitational wave (GW) by the LIGO-VIRGO collaboration and its electromagnetic counterparts by ~ 70 ground and space based detectors [1]. All these observations strongly suggest that this event (GW170817) is associated with a system of binary neutron star (BNS) merger.

While implications of this new data is being analyzed thoroughly in the context of the internal structure of a Neutron star (NS) [2–11], we are still far from definitive answers. It has been shown that with more events of this type, we will be able to constrain the NS parameters with better accuracy which in turn, will allow us to probe dense matter physics in precise detail [12]. The equation of state (EOS) of matter has distinct effects on every stage of BNS evolution. During the inspiral phase, the EOS-dependent tidal deformability parameter relates the quadrupolar response of a star with the external static tidal field exerted by its companion in the binary. Flanagan and Hinderer have shown how this parameter can influence the inspiral GW signal [13–15]. From the data of GW170817, LIGO-VIRGO collaboration [1] obtained an upper limit for the dimensionless tidal deformability of a $1.4M_{\odot}$ NS as $\Lambda(1.4M_{\odot}) \leq 800$. The impact of this constraint has recently been studied on pure hadronic NS [8], quark stars [9] as well as hybrid stars [11] having hadron-quark phase transition (PT) in the stellar interior.

In this article we investigate the consequence of the tidal deformability constraints on the properties of hybrid stars. Unlike Ref. [11], we construct EOS with PT from hadronic matter to quark matter via Gibbs' construction where the PT proceeds through the appearance of a quark-hadron mixed phase [16, 17]. The formation of mixed phase is favored when the surface tension between nuclear and quark matter is small ($\sigma \lesssim 40$ MeV/fm 2) [18, 19]. So far, the calculation of σ is very much model dependent and can have values in the range ~ 5 –300 MeV/fm 2 [18–24]. For higher values of σ the phase transition is sharp and is treated with the prescription of Maxwell construction. As the value of σ is not settled yet both the scenarios (Maxwell and Gibbs') are plausible. We adopt here the Gibbs' construction. In this case the outer part of the compact star contains hadronic matter, whereas the core can have either pure quark matter or the hadron-quark mixed phase - giving rise to a hybrid star.

The article is organized as follows. In the next section we present the details of EOS and the calculation of tidal deformability of hybrid stars. The effect of the tidal deformability constraint coming from GW170817 on the EOS of hybrid stars are investigated in Section III. Finally, we summarize and conclude in Section IV.

II. SET UP

To construct the EOS of nuclear matter we adopt the relativistic mean-field (RMF) approach [25, 26] where interaction between nucleons are described by the exchange of σ , ω and ρ mesons. We use three widely used parameter sets: NL3 [27] which includes non-linear self-interaction of σ -mesons, TM1 [28] that has self-interacting terms for both σ and ω mesons and NL3 $\omega\rho$ [29] where self-interaction of σ mesons and coupling between ω and ρ mesons are considered. It was shown in Ref. [30] that the calculation of NS properties (especially radius) is unambiguous if the EOS is unified in the sense that the EOS of crust and core are obtained using the same many-body theory. As Λ is highly sensitive to radius ($\Lambda \sim R^5$), we take EOS of inner crusts from Ref. [31] where they were calculated using the same parameters sets. For the outer crust we take DH EOS [32]. As most part of the outer crust is determined from the experimentally measured masses, the choice of outer crust does not have any significant impact on the observables.

For the description of quark matter we use the modified MIT bag model described by the Grand potential [33]:

$$\Omega_{QM} = \sum_i \Omega_i^0 + \frac{3\mu^4}{4\pi^2} (1 - a_4) + B_{\text{eff}}, \quad (1)$$

where Ω_i^0 stand for the Grand potentials of non-interacting Fermi gases of up (u), down (d) and strange (s) quarks as well as electrons. The last two terms include the strong interaction correction and the nonperturbative QCD effects via two effective parameters a_4 and B_{eff} , respectively with $\mu (= \mu_u + \mu_d + \mu_s)$ being the baryon chemical potential of quarks.

We consider the PT from hadronic matter to quark matter via Gibbs' construction [17], where a mixed phase of hadronic and quark matter is formed between pure hadronic and quark phases.

At the initial stage of the inspiral signal from a coalescing binary neutron star system,

the tidal effects on a star can be taken at the linear order as,

$$Q_{ij} = -\lambda \mathcal{E}_{ij}, \quad (2)$$

where Q_{ij} is the induced quadrupole moment of the star and \mathcal{E}_{ij} can be assumed as external static tidal field exerted by the partner. The parameter λ is related to the dimensionless, $\ell = 2$, electric-type tidal love number as,

$$\lambda = \frac{2}{3} k_2 R^5, \quad (3)$$

where, R is the radius of the star. We calculate k_2 and subsequently λ following the framework developed by Hinderer and collaborators [14, 15]. However, in our present calculations, we use dimensionless tidal deformability Λ (defined as : $\Lambda = \lambda/M^5$, where M is the mass of the star and we assume $G = c = 1$) which is a direct observable quantity from the GW signal. The accumulated phase contribution due to the deformation from both the stars is imbibed in inspiral signal as the combined dimensionless tidal deformability which is given by ,

$$\tilde{\Lambda} = \frac{16}{13} \frac{(M_1 + 12M_2) M_1^4 \Lambda_1 + (M_2 + 12M_1) M_2^4 \Lambda_2}{(M_1 + M_2)^5}, \quad (4)$$

where, Λ_1 and Λ_2 are the individual deformability associated with the stars with masses M_1 and M_2 respectively [34].

III. RESULTS AND DISCUSSION

We construct the EOS of hybrid stars via Gibbs' construction as described in the previous section. For the hadronic part we take three different parameter sets NL3, TM1 and NL3 $\omega\rho$ all of which give maximum NS masses (M_{\max}) more than $2M_{\odot}$ and are therefore compatible with the constraint of $M_{\max} = 2.01 \pm 0.04M_{\odot}$ obtained from observation [35]. On the other hand, we generate a large number of quark matter EOS represented by the different values of $B_{\text{eff}}^{1/4}$ and a_4 . We then combine all three hadronic EOS with all quark EOS via Gibbs' construction. However, we exclude those EOS where the starting density (n_{crit}) of the mixed phase is lower than the crust-core transition density (n_{cctd}).

In Fig. 1, we show the maximum masses of hybrid stars for all EOS considered here. Similar figures were also obtained in Ref. [33] for NL3 and TM1 parameter sets. However, our figures for these two parameter sets are not identical to that of Ref. [33] at small B_{eff} .

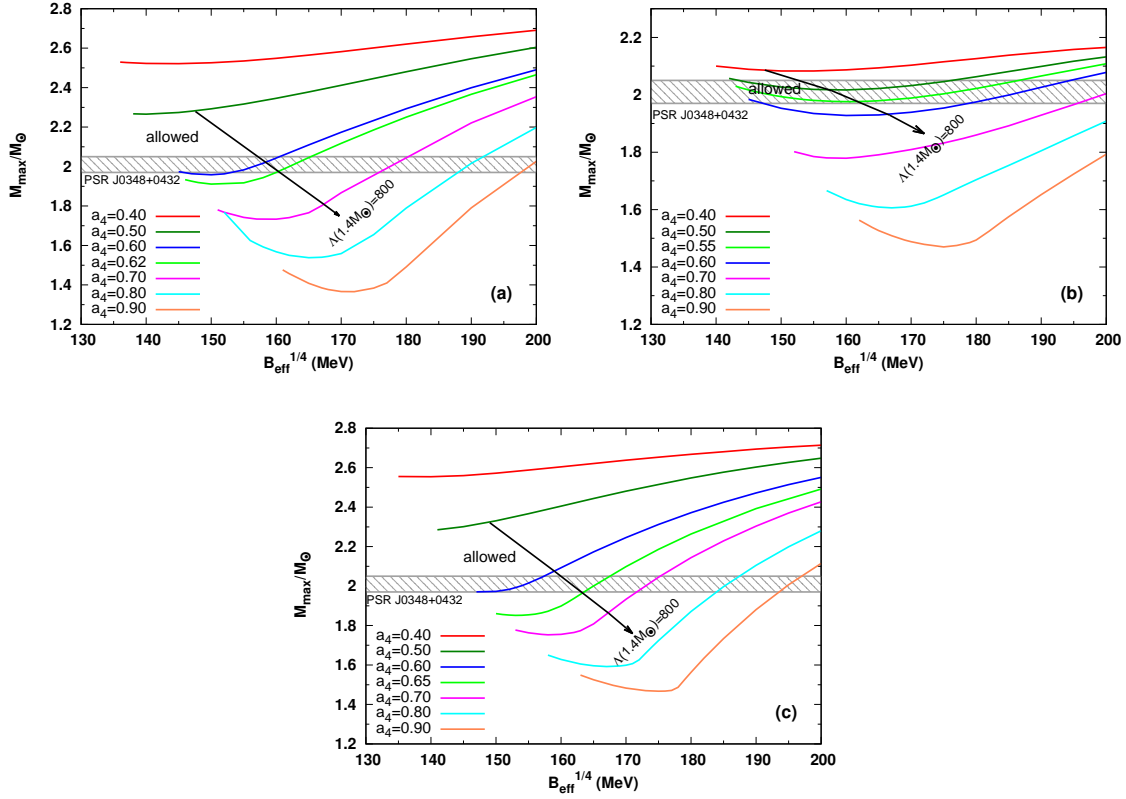


FIG. 1. Maximum masses of hybrid stars as a function of $B_{\text{eff}}^{1/4}$ and a_4 for (a) NL3, (b) TM1 and (c) NL3 $\omega\rho$ parameter sets.

This is because of the inclusion of the crust and excluding the EOS with $n_{\text{crit}} < n_{\text{cctd}}$. We also show the results for NL3 $\omega\rho$ which were not presented earlier. For all three parameter sets we see that the observation of $\sim 2M_{\odot}$ NS already constraint the $(B_{\text{eff}}^{1/4}, a_4)$ parameter space, considerably.

Next, we calculate the tidal deformabilities of all the EOS of hybrid stars as well as pure hadronic stars considered here. In Fig. 2 we plot the individual tidal deformabilities Λ_1 and Λ_2 of both the compact stars associated with the binary merger event GW170817. For a given EOS, we calculate Λ_1 and Λ_2 by varying the mass of the primary star between $M_1 = 1.365 - 1.600M_{\odot}$ and that of secondary star in the range $M_2 = 1.170 - 1.365M_{\odot}$, so that the combinations of M_1 and M_2 give the chirp mass $\mathcal{M} = (M_1 M_2)^{3/5} (M_1 + M_2)^{-1/5} = 1.188M_{\odot}$ of GW170817 [1]. In all the plots of Fig. 2, we show the results for only those EOS that gives M_{max} consistent with the observation [35]. From the figure it is seen that only NL3 $\omega\rho$ EOS is close to the 90% probability contour set by the event GW170817, by assuming low-

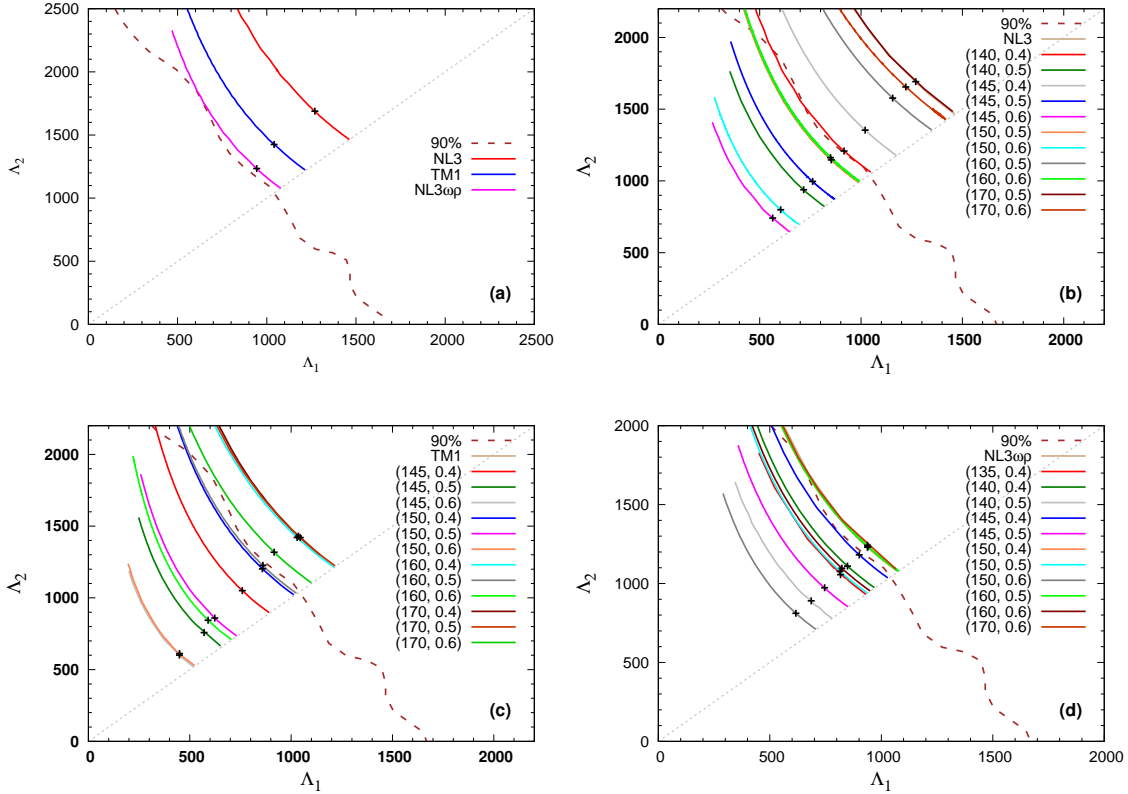


FIG. 2. Tidal deformabilities Λ_1 and Λ_2 corresponding to the high mass M_1 and low mass M_2 components of the binary system for the event GW170817 calculated for (a) pure hadronic stars and hybrid stars with (b)NL3, (c)TM1 and (d)NL3 $\omega\rho$ parameter sets.

spin priors $|\chi| \leq 0.05$ [1]. Other two EOS (NL3 and TM1) lie far from the contour and are therefore excluded. Interestingly, when PT from hadronic matter to quark matter via Gibbs' construction is included we find several EOS corresponding to different $(B_{\text{eff}}^{1/4}, a_4)$ combinations satisfy the constraint set by the contour, for all three hadronic models.

In Fig. 2 we also mark the points (Λ_1, Λ_2) that correspond to $M_1 = 1.4M_\odot$, with cross signs. Careful observation reveals that not all the EOS which are inside the 90% contour satisfy the constraint $\Lambda(1.4M_\odot) \leq 800$ derived for the event GW170817 in Ref. [1]. To see the consequence of this constraint on the EOS of hybrid stars we include it (showed by long arrow) in all the plots of Fig. 1. It is remarkable to find that the constraint reduce the $(B_{\text{eff}}^{1/4}, a_4)$ parameter space (marked with "allowed" in the plots) significantly in all three cases. The maximum allowed values for $B_{\text{eff}}^{1/4}, a_4$ are given in Table I.

Next, we investigate the effect of the combined tidal deformability constraint as derived for the event GW170817 assuming low-spin scenario [1], on the EOS of hybrid stars. We

TABLE I. Maximum allowed values of $B_{\text{eff}}^{1/4}$ and a_4 obtained from Fig. 1.

| Model | $B_{\text{eff}}^{1/4}$ (MeV) | a_4 |
|------------------|------------------------------|-------|
| NL3 | 160 | 0.62 |
| TM1 | 162 | 0.55 |
| NL3 $\omega\rho$ | 163 | 0.65 |

 TABLE II. Parameters for fit of $\tilde{\Lambda}$ as a function of $R_{1.4}$ and resulting bounds.

| $M_1 = M_2 = 1.365M_{\odot}$ | | | | | |
|--------------------------------|---------|----------|---------|----------------|------------------------------|
| Model | a | b | c | $R_{1.4}$ (km) | $B_{\text{eff}}^{1/4}$ (MeV) |
| NL3, $a_4 = 0.5$ | 46517.4 | -7012.76 | 269.057 | 13.93 | 151.7 |
| NL3, $a_4 = 0.6$ | 30816.9 | -4814.86 | 192.145 | 13.95 | 161.0 |
| NL3 $\omega\rho$, $a_4 = 0.5$ | 71678.7 | -10904.6 | 419.515 | 13.73 | 156.0 |
| NL3 $\omega\rho$, $a_4 = 0.6$ | 40527.3 | -6366.3 | 254.227 | 13.73 | 164.0 |

consider the case of equal mass with $M_1 = M_2 = 1.365M_{\odot}$ as well as the case of unequal mass with $M_1 = 1.60M_{\odot}$, $M_2 = 1.17M_{\odot}$. The corresponding bounds are $\tilde{\Lambda} \leq 1040$ and $\tilde{\Lambda} \leq 800$, respectively. In Fig. 3, we use the bound for equal mass case to predict the radius of a $1.4M_{\odot}$ star as well as $B_{\text{eff}}^{1/4}$ for two allowed values of a_4 (see Fig. 1) and for parameter sets NL3 and NL3 $\omega\rho$. It is interesting to see that for both the parameter sets the bounds on $R_{1.4}$ (shown by vertical dashed lines) are independent of a_4 and are given by $R_{1.4} \leq 13.9$ km and $R_{1.4} \leq 13.7$ km for NL3 and NL3 $\omega\rho$, respectively. The values of $R_{1.4}$ and corresponding bounds on $B_{\text{eff}}^{1/4}$ are listed in the last two columns of Table II. The values of $\tilde{\Lambda}$ can easily be fitted with a quadratic function of the form:

$$\tilde{\Lambda}_{\text{fit}} = a + bR_{1.4} + cR_{1.4}^2. \quad (5)$$

The fit parameters are given in the first three columns of Table II. We include these fits in Fig. 3. The predicted bounds for $R_{1.4}$ can also be calculated by putting $\tilde{\Lambda} = 1040$ in eq. (5) and the obtained values are in good agreement with the values obtained from the figures (Fig. 3). It is seen from the Table II that the limiting value of $R_{1.4}$ for NL3 is only slightly higher than that of NL3 $\omega\rho$. However, the upper limit on $B_{\text{eff}}^{1/4}$ is higher for NL3 $\omega\rho$ than NL3 by ~ 4 MeV and 3 MeV for $a_4 = 0.5$ and $a_4 = 0.6$, respectively.

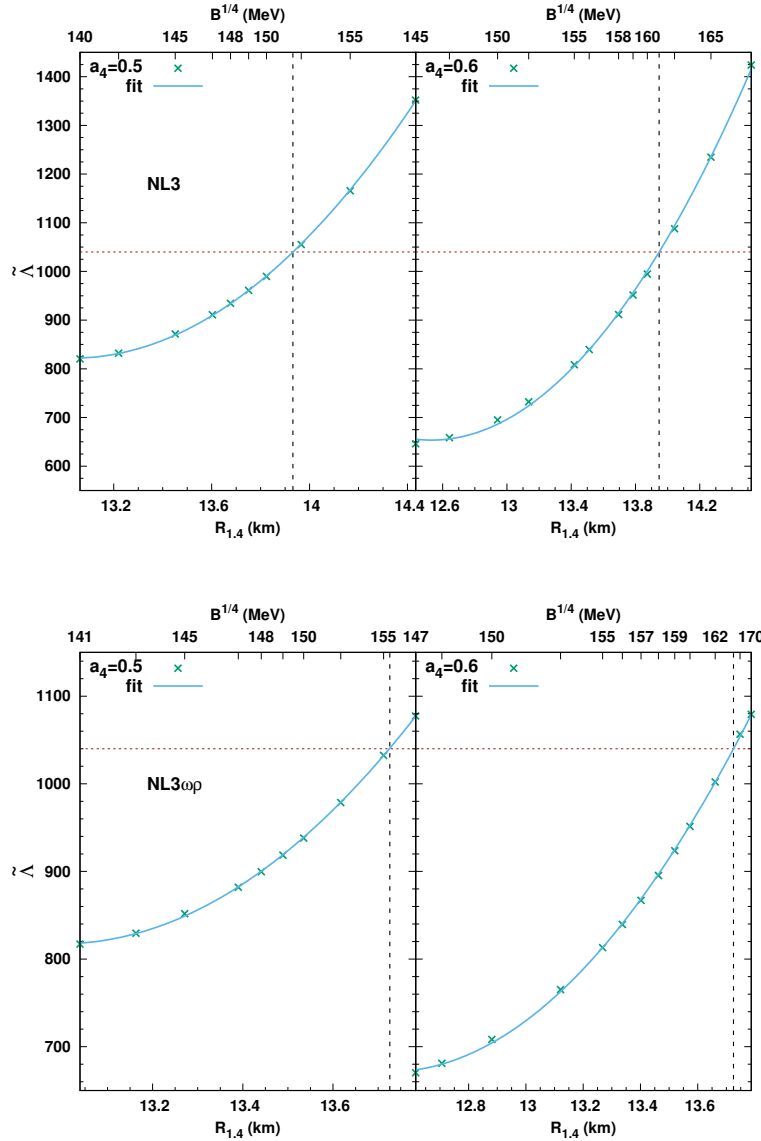


FIG. 3. The calculated values of $\tilde{\Lambda}$ for the equal mass scenario as a function of radius of a $1.4M_{\odot}$ star $R_{1.4}$ (lower x-axis) and $B_{\text{eff}}^{1/4}$ (upper x-axis) for parameter sets NL3 (upper panel) and NL3 $\omega\rho$. The solid line is the fit given by Eq. (5). The horizontal dashed line at $\tilde{\Lambda}=1040$ is the constraint from GW170817 [1]. The vertical line represents the upper bound on $R_{1.4}$ and $B_{\text{eff}}^{1/4}$ due to this constraint.

We perform similar analysis for the unequal mass case and obtain bound on $R_{1.6}$ and $B_{\text{eff}}^{1/4}$. The plots including the fits are shown in Fig. 4. The fit parameters and the resulting bounds from the $\tilde{\Lambda} = 800$ constraint are shown in Table III. In this case both the parameter sets predict similar bounds on $R_{1.6}$ and $B_{\text{eff}}^{1/4}$.

TABLE III. Fit parameters and bounds for unequal mass scenario.

| $M_1 = 1.60M_\odot, M_2 = 1.17M_\odot$ | | | | | |
|--|---------|----------|---------|----------------------|-----------------------|
| Model | a | b | c | $R_{1.6}(\text{km})$ | $B^{1/4}(\text{MeV})$ |
| NL3, $a_4 = 0.5$ | 53151.5 | -8069.29 | 310.702 | 13.35 | 142.0 |
| NL3, $a_4 = 0.6$ | 25530.6 | -4095.41 | 168.004 | 13.35 | 154.2 |
| NL3 $\omega\rho$, $a_4 = 0.5$ | 45123.8 | -6926.73 | 270.201 | 13.32 | 143.2 |
| NL3 $\omega\rho$, $a_4 = 0.6$ | 17894.3 | -2931.8 | 123.759 | 13.32 | 154.6 |

 TABLE IV. Range of allowed values of $B_{\text{eff}}^{1/4}$.

| NL3 | | |
|------------------|--|--|
| a_4 | $M_1 = M_2 = 1.365M_\odot$ | $M_1 = 1.60M_\odot, M_2 = 1.17M_\odot$ |
| 0.5 | $138 \leq B_{\text{eff}}^{1/4} \leq 152$ | $138 \leq B_{\text{eff}}^{1/4} \leq 142$ |
| 0.6 | $145 \leq B_{\text{eff}}^{1/4} \leq 161$ | $145 \leq B_{\text{eff}}^{1/4} \leq 154$ |
| NL3 $\omega\rho$ | | |
| a_4 | $M_1 = M_2 = 1.365M_\odot$ | $M_1 = 1.60M_\odot, M_2 = 1.17M_\odot$ |
| 0.5 | $141 \leq B_{\text{eff}}^{1/4} \leq 156$ | $141 \leq B_{\text{eff}}^{1/4} \leq 143$ |
| 0.6 | $147 \leq B_{\text{eff}}^{1/4} \leq 164$ | $147 \leq B_{\text{eff}}^{1/4} \leq 155$ |

When we combine the lower bound on $B_{\text{eff}}^{1/4}$ set by the requirement that $n_{\text{crit}} > n_{\text{cctd}}$ with the upper bounds on $B_{\text{eff}}^{1/4}$ obtained above using the $\tilde{\Lambda}$ constraints coming from the event GW170817, we get the range of values for $B_{\text{eff}}^{1/4}$ given in the Table IV. It is seen from the table that the unequal mass scenario put more stringent constraint on the values of $B_{\text{eff}}^{1/4}$ for both values of a_4 . Particularly, for $a_4 = 0.5$ allowed $B_{\text{eff}}^{1/4}$ values are found to lie within a very narrow range.

The first model-independent measurement of neutron skin thickness is provided by the Lead Radius Experiment PREX as $R_{\text{skin}}^{208} = 0.33^{+0.16}_{-0.18}$ fm [36]. The result is not very useful because of the large statistical error. However, the upcoming PREX-II experiment is supposed to reduce the uncertainty to 0.06 fm. On the other hand, the calculated values of R_{skin}^{208} within NL3 and NL3 $\omega\rho$ parameter sets are 0.28 fm and 0.21 fm, respectively. If PREX-II gives a value closer to the current central value of 0.33 fm NL3 $\omega\rho$ would be excluded. However, NL3 might be consistent with the measured R_{skin}^{208} as well as the bound set by the event

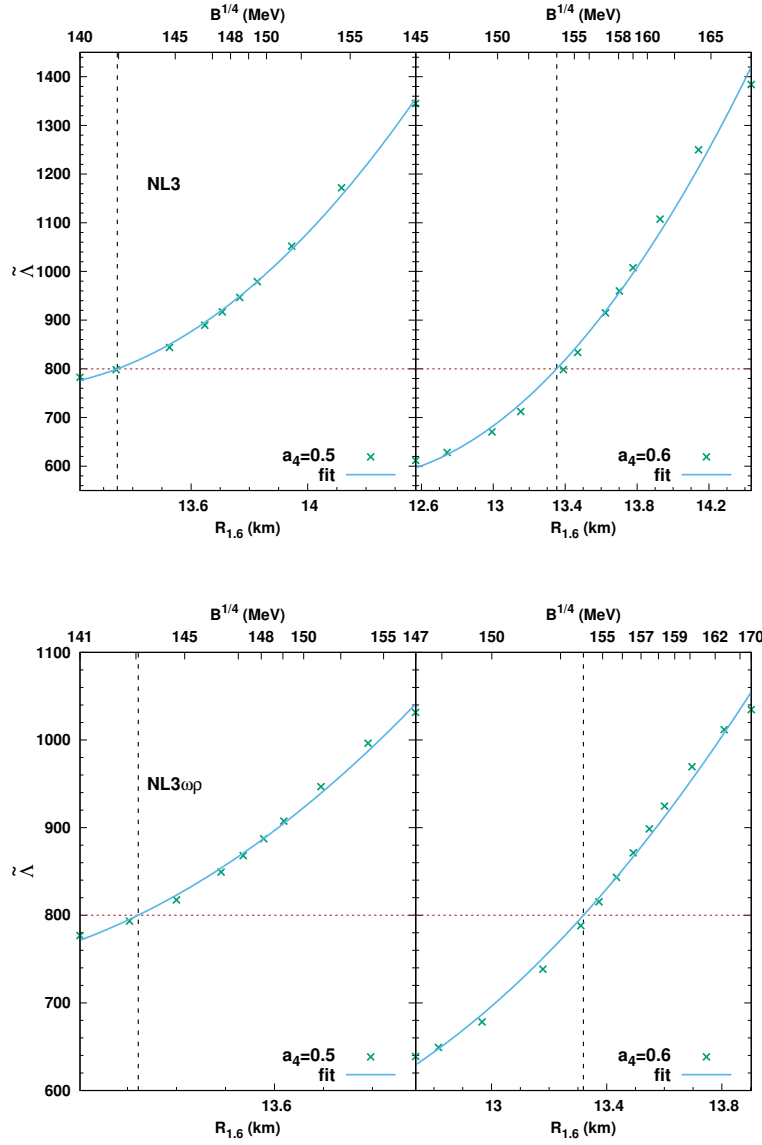


FIG. 4. Similar to Fig. 3 but for the unequal mass scenario and as a function of radius of a $1.6M_{\odot}$ star $R_{1.6}$ (lower x-axis). The horizontal dashed line at $\tilde{\Lambda}=800$ is the constraint from GW170817 [1]. The vertical line represents the corresponding upper bound on $R_{1.6}$ and $B_{\text{eff}}^{1/4}$.

GW170817 only if the PT to quark matter is taken into consideration, as already indicated in Ref. [8].

IV. SUMMARY

We have investigated here how the tidal deformability bound given by the binary NS merger event GW170817 constraints the EOS of hybrid stars. The EOS of hybrid stars are constructed via the Gibbs' construction through the formation of hadron-quark mixed phase. For the hadronic part we employ the RMF model with three widely used parameter sets: NL3, TM1 and NL3 $\omega\rho$, whereas the quark matter is described with the help of the modified bag model. It is found that pure hadronic EOS for all three parameters sets are excluded as they give values of Λ considerably larger than the constraint $\Lambda(1.4M_\odot) \leq 800$, set by GW170817. They also lie outside the 90% contour in the (Λ_1, Λ_2) plane. Interestingly, when the PT to quark matter via the formation of mixed phase is considered, we find several combinations of $B_{\text{eff}}^{1/4}$ and a_4 that are consistent with the above constraints for all three cases. However, imposition of constraints $\Lambda(1.4M_\odot) \leq 800$ and $M_{\text{max}} = 2.01 \pm 0.04M_\odot$ together leads to significant reduction of $(B_{\text{eff}}^{1/4}, a_4)$ parameter space. We have also investigated the effect of combined tidal deformability constraints $\tilde{\Lambda} \leq 1040$ and $\tilde{\Lambda} \leq 800$ for equal and unequal mass scenarios, respectively derived from the event GW170817 assuming low spin priors. Both these bounds found to put stringent constraints on the allowed values of $B_{\text{eff}}^{1/4}$ and a_4 . For the equal mass case we have obtained bound for radius of a $1.4M_\odot$ hybrid stars as $R_{1.4} \leq 13.9$ km for NL3 and $R_{1.4} \leq 13.7$ km for NL3 $\omega\rho$. Similarly, the unequal mass scenario gives bound on the radius of a $1.6M_\odot$ star as $R_{1.6} \lesssim 13.3$ km for both NL3 and NL3 $\omega\rho$. We also observed that if the upcoming PREX-II experiment measures relatively larger $\text{Pb}_{\text{skin}}^{208}$, EOS of hybrid stars with NL3 $\omega\rho$ would be excluded but NL3 hybrid stars would survive.

ACKNOWLEDGMENTS

P. Char acknowledges support from the Navajbai Ratan Tata Trust.

[1] B. P. Abbott *et al.* (LIGO Scientific and Virgo Collaborations), Phys. Rev. Lett. **119**, 161101 (2017).

- [2] M. Shibata, S. Fujibayashi, K. Hotokezaka, K. Kiuchi, K. Kyutoku, Y. Sekiguchi, and M. Tanaka, arXiv:1710.07579 [astro-ph.HE].
- [3] A. Bauswein, O. Just, N. Stergioulas, and H.-T. Janka, arXiv:1710.06843 [astro-ph:HE].
- [4] L. Rezzolla, E. R. Most, and L. R. Weih, arXiv:1711.00314 [astro-ph.HE]
- [5] M. Ruiz, S. L. Shapiro, and A. Tsokaros, arXiv:1711.00473 [astro-ph.HE].
- [6] E. Annala, T. Gorda, A. Kurkela, and A. Vuorinen, arXiv:1711.02644 [astro-ph.HE].
- [7] B. Margalit and B. D. Metzger, arXiv:1710.05938v2 [astro-ph.HE].
- [8] F. J. Fattoyev, J. Piekarewicz, and C. J. Horowitz, arXiv:1711.06615 [astro-ph.HE].
- [9] E. Zhou, X. Zhou, and A. Li, arXiv:1711.04312 [astro-ph.HE].
- [10] D. Radice, A. Perego, and F. Zappa, arXiv:1711.03647 [astro.ph-HE]
- [11] V. Paschalidis, K. Yagi, D. Alvarez-Castillo, D. B. Blaschke and A. Sedrakian, arXiv:1712.0045 [astro-ph.HE].
- [12] S. Bose, K. Chakravarti, L. Rezzolla, B. S. Sathyaprakash, K. Takami, arXiv:1705.10850 [gr-qc].
- [13] É. É Flanagan, and T. Hinderer, Phys. Rev. D **77**, 021502 (2008).
- [14] T. Hinderer, Astrophys. J. **677**, 1216 (2008).
- [15] T. Hinderer, B. D. Lackey, R. N. Lang and J. S. Read, Phys. Rev. D **81**, 123016 (2010)
- [16] N. K. Glendenning, *Compact Stars, Nuclear Physics, Particle Physics, and General Relativity*, 2nd ed. (Springer-Verlag, New York, 2000).
- [17] N. K. Glendenning, Phys. Rev. D. **46**, 1274 (1992).
- [18] M. G. Alford, K. Rajagopal, S. Reddy, and F. Wilczek, Phys. Rev. D **64**, 074017 (2001)
- [19] D. N. Voskresensky, M. Yasuhira, and T. Tatsumi, Nucl. Phys. A **723**, 291 (2003).
- [20] L. F. Palhares and E. S. Fraga, Phys. Rev. D **82**, 125018 (2010).
- [21] M. B. Pinto, V. Koch, and J. Randrup, Phys. Rev. C **86**, 025203 (2012).
- [22] B. W. Mintz, R. Stiele, R. O. Ramos, and J. Schaffner-Bielich, Phys. Rev. D **87**, 036004 (2013).
- [23] G. Lugones, A. G. Grunfeld, and M. Al Ajmi, Phys. Rev. C **88**, 045803 (2013).
- [24] N. Yasutake, R. Lastowiecki, S. Benic, D. Blaschke, T. Maruyama, and T. Tatsumi, Phys. Rev. C **89**, 065803 (2014).
- [25] J. D. Walecka, Ann. Phys. **83**, 491 (1974).
- [26] B. D. Serot, Phys. Lett. **86B**, 146 (1979).

- [27] G. A. Lalazissis, J. König, and P. Ring, Phys. Rev. C **55**, 540 (1997).
- [28] Y. Sugahara, and H. Toki, Nucl. Phys. A **579**, 557 (1994).
- [29] C. J. Horowitz, and J. Piekarewicz, Phys. Rev. Lett. **86**, 5647 (2001); Phys. Rev. C **64**, 062802 (2001).
- [30] M. Fortin, Ad. R. Raduta, F. Gulminelli, J. L. Zdunik, P. Haensel and M. Bejger, Phys. Rev. C. **94**, 035804 (2016).
- [31] F. Grill, H. Pais, C. Providécia, and Isaac Vidaña, Phys. Rev. C 90, 045803 (2014).
- [32] P. Haensel, A. Y. Potekhin, and D. G. Yakovlev, *Neutron Stars 1, Equation of State and Structure*, Springer (2007).
- [33] S. Weissenborn, I. Sagert, G. Pagliara, M. Hempel, and J. Schaffner-Bielich, Astrophys. J. **740**, L14 (2011).
- [34] M. Favata, Phys. Rev. Lett. **112**, 101101 (2014)
- [35] J. Antoniadis et al., Science **340**, 1233232 (2013).
- [36] S. Abrahamyan *et al.*, Phys. Rev. Lett. **108**, 112502 (2012).